This manuscript was accepted by Appl. Phys. Lett. Click here to see the version of record.

AIP Publishing

Carrier scattering induced linewidth broadening in in-situ P-doped Ge layers on Si

S. A. Srinivasan,[1,2,3,a)] C. Porret,[1] M. Pantouvaki,[1] Y. Shimura,[1,4] P. Geiregat,[2,3,5] R. Loo,[1] J. Van Campenhout,[1] and D. Van Thourhout[1,2,3,b)]

[1)] *Imec, Kapeldreef 75, Heverlee-3001, Belgium*
[2)] *Photonics Research Group, Dept. of Information Technology, Ghent University-imec, Technologiepark-Zwijnaarde 16 iGent, Ghent-9052, Belgium*
[3)] *Center for Nano- and Biophotonics, Ghent University, Technologiepark-Zwijnaarde 16 iGent, Ghent-9052, Belgium*
[4)] *Current address: Shizuoka University, Hamamatsu 432-8001, Japan*
[5)] *Physics and Chemistry of Nanostructures, Ghent Univeriesty, 9000-Ghent, Belgium*

(Dated: 22 September 2018)

Highly P doped Ge layers are proposed as a material to realize an on-chip laser for optical interconnect applications. In this work, we demonstrate that these donor impurities have a dramatic impact on the excess carrier lifetime and introduce detrimental many-body effects such as linewidth broadening in the gain medium. Linewidth broadening $\Gamma_{opt} = 10$ meV for undoped Ge and $\Gamma_{opt} \geq 45$ meV for Ge with doping level up to 5.4×10^{19} cm^{-3}, were extracted using photoluminescence spectroscopy and pump-probe spectroscopy. In addition, we observed that the excess carrier lifetime (τ_c) drops by more than an order of magnitude from 3 ns in undoped Ge to < 0.3 ns in doped Ge.

ACCEPTED MANUSCRIPT

Silicon photonics exploits the CMOS infrastructure and the asociated economies of scale to realize robust and cost-effective active[1,2] and passive devices[3,4] co-integrated in complex photonics integrated circuits for short-reach interconnect applications[5]. Within this platform, Germanium (Ge) has been extensively used as optical absorption material in high speed photodetectors and electro-absorption modulators exploiting the presence of the direct band gap around 0.8 eV[1,2]. However, Ge is also an inefficient light emitter due to the presence of an indirect band gap located at energies lower than the direct band gap. To increase the efficiency of the light source, high n-type doping of Ge with P atoms is considered[6]. Electrically driven Ge lasers that exploit this mechanism have been previously demonstrated but exhibit high threshold current densities in the range of 280-510 kA/cm^2 for doping levels of 3-4$\times10^{19}$ cm^{-3} due to reduced carrier lifetime[7–10]. In addition to a reduction in carrier lifetime, linewidth broadening effects have a crucial impact on the expected gain spectrum of highly doped Ge layers as we will show in this work. This is done by comparing the shape and full width at half maximum (FWHM) of photoluminescence (PL) signals of doped and undoped Ge layers grown on Si. In addition to PL studies, we also perform pump-probe spectroscopy where spectral changes of the absorption coefficient under short pulse optical pumping are investigated. We observe broadening of the PL spectra and suppression of optical bleaching effects and support these observations with a joint density of states model that allows to extract the broadening width Γ_{opt}.

The investigated set of samples consists of undoped and doped Ge films epitaxially grown on Si using Reduced Pressure Chemical Vapour Deposition (RPCVD)[6]. Undoped Ge films were obtained by growing a 1 μm thick Ge buffer on a 300 mm Si (001) substrate and thinning it down to 0.6 μm using chemical mechanical polishing (CMP). This Ge buffer layer is 0.2% biaxially tensile strained (originating from the mismatch of the thermal expansion coefficients of Ge and Si) as measured by X-ray diffraction. A few of the 0.6 μm undoped Ge films were further thinned down to 0.2 μm, before growing P-doped Ge layers on top using Ge_2H_6 and PH_3 as precursors[6]. The doped layers were later rapid thermal annealed at 700°C for 30 s in order to activate the dopants and diffuse them into the underlying 0.2 μm thick Ge buffer[11]. Using this strategy, active doping levels of 2.7×10^{19} cm^{-3}, 4.5×10^{19} cm^{-3} and 5.4×10^{19} cm^{-3} were obtained as verified using secondary ion mass spectroscopy (SIMS) and micro Hall effect (MHE) measurements. The atomic P concentration profile measured using SIMS was uniform and constant across the Ge layer.

Photoluminescence signals from these layers were obtained using a micro photoluminescence (μPL) setup at room temperature with a continuous wave laser of 0.532 μm emission wavelength and intensity of 30 kW/cm^2 as the pump source. The photoluminescence signal from

TABLE I. Samples investigated and the corresponding broadening width (Γ_{opt}) as extracted in this work.

Sample Name	Chemical P Conc. (cm^{-3})	Active P Conc.(cm^{-3})	Γ_{Lorr} (meV)	Γ_{Gauss} (meV)
A	N/A	N/A	10 ± 3	10 ± 3
B	3.0×10^{19}	2.7×10^{19}	50 ± 5	53 ± 5
C	5.6×10^{19}	4.5×10^{19}	52.5 ± 5	58 ± 5
D	7.2×10^{19}	5.4×10^{19}	50 ± 5	53 ± 5

[a)] Electronic mail: ashwyn.srinivasan@imec.be
[b)] Electronic mail: dries.vanthourhout@ugent.be

This manuscript was accepted by Appl. Phys. Lett. Click here to see the version of record.
AIP Publishing

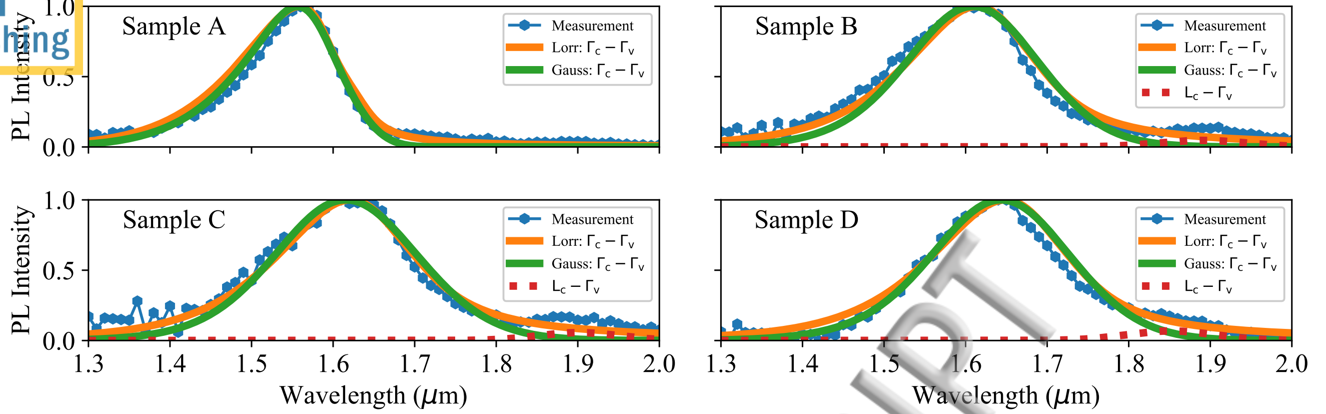

FIG. 1. Normalized room temperature PL spectra of all samples listed in Table I, which have doping levels increasing from undoped (Sample A) to 5.4×10^{19} cm^{-3} (Sample D). The measurement results are for a continuous wave pumping intensity of 30 kW/cm^2 at 0.532 μm. A small peak (dashed curve) at longer wavelength is visible for the doped samples and corresponds to the $L_C - \Gamma_V$ indirect recombination process.

the sample was detected using a liquid nitrogen cooled Ex-InGaAs detector covering the wavelength range from 1.3 μm to 2.0 μm. In addition to the PL measurements, pump-probe spectroscopy was carried out to track the carrier dynamics in Ge as a function of time and photon wavelength. The pump probe spectroscopy setup uses 100 fs pump pulses with a repetition rate of 1 kHz, centered at a wavelength of 1.3 μm. The temporal resolution of the setup is 150 fs. A broadband signal from 0.85 μm to 1.7 μm wavelength was used as the probe. The intensity of the pump pulses was varied from 28 to 140 mW/cm^2. The absorption of the pump pulses in Ge generates a high density of photo-excited carriers that decay in time due to radiative and non-radiative mechanisms. These photoexcited carriers affect the spectral shape of the transmitted broadband probe beam through free-carrier absorption (FCA) and the optical bleaching effect (OBE). This change in transmitted light is converted to a change in absorption coefficient. By fitting the spectral shape of the change in absorption coefficient measured in the pump-pulse spectroscopy setup and the PL signal from the doped and undoped Ge layers, we estimate the strength of the linewidth broadening present in doped and undoped samples. Moreover, the temporal response of the carrier dynamics allows us to estimate the carrier lifetime in these layers.

The room temperature PL spectra of undoped and doped Ge layers are shown in Fig. 1. The dominant emission peak in these spectra corresponds to the $\Gamma_c - \Gamma_v$ direct transition. Comparing the spectra from doped and undoped Ge, it is obvious that this peak shifts to lower energies for the doped samples, which is attributed to dopant-induced band gap narrowing[12,13]. In the doped samples, a second emission peak can be observed at photon wavelengths between 1.8 μm and 1.9 μm. This peak is attributed to the $L_c - \Gamma_v$ indirect transition originating due to the presence of dopants[9]. Even aside from this second peak, the measured spectra for the doped layers (Samples B to D) are significantly broader than that of the undoped Ge layer (Sample A). Such broadening was also observed on doped Ge layers grown on 1 μm thick Ge buffer that did not receive CMP. We believe this is related to carrier scattering due to dopant incorporation in Ge. But we restrict our studies to uniformly doped Ge layers listed in Table I to ease our modelling efforts. In order to study the extent of the broadening in these layers, we fit the measured PL spectra using the van Roosbroeck-Schockley (vR-S) relation under quasi-equilibrium:

$$R_{sp}(\hbar\omega) = \frac{(\hbar\omega)^2 n_{Ge}^2}{(\pi c)^2 \hbar^3} \alpha_{Direct}(\hbar\omega) \frac{f_c(\hbar\omega)(1 - f_v(\hbar\omega))}{f_v(\hbar\omega) - f_c(\hbar\omega)} \quad (1)$$

This equation relates the photon emission rate $R_{sp}(\hbar\omega)$ with the absorption coefficient $\alpha_{Direct}(\hbar\omega)$. The absorption coefficient, without the presence of any carrier-carrier scattering or carrier-phonon scattering that introduce linewidth broadening, is expressed as:

$$\alpha(\hbar\omega) = \frac{\pi e^2 |\hat{e} \cdot \rho_{cv}|}{n_{Ge} c \epsilon_o \omega m_o^2} \rho(\hbar\omega - E_g)\big(f_v(\hbar\omega) - f_c(\hbar\omega)\big) \quad (2)$$

with

$$\rho(\hbar\omega - E_g) = \frac{1}{2\pi^2} \frac{2m_r^*}{\hbar^2}^{3/2} \sqrt{\hbar\omega - E_g} \quad (3)$$

This absorption coefficient assumes a simple quadratic behaviour for the joint density of states, represented as $\rho(\hbar\omega - E_g)$[14]. In this simple absorption model we neglect exciton effects, as commonly done in the literature[15]. We can include carrier scattering physics by modifying the absorption coefficient to:

$$\alpha_{Direct}(\hbar\omega) = \int_0^\infty \alpha(E) L(\hbar\omega - E) \delta E \quad (4)$$

ACCEPTED MANUSCRIPT

This manuscript was accepted by Appl. Phys. Lett. Click here to see the version of record.
AIP Publishing

$$\mathrm{L}(\hbar\omega - \mathrm{E}) = \frac{1}{\pi}\frac{\Gamma_{\mathrm{Lorr}}/2}{(\Gamma_{\mathrm{Lorr}}/2)^2 + (\hbar\omega - \mathrm{E})^2} \quad (5)$$

or

$$\mathrm{L}(\hbar\omega - \mathrm{E}) = \frac{1}{\sigma\sqrt{2\pi}}\exp\left[-\frac{(\hbar\omega - \mathrm{E})^2}{2\sigma^2}\right] \quad (6)$$

with $\sigma = 0.425 \times \Gamma_{\mathrm{Gauss}}$. The lineshape function $\mathrm{L}(\hbar\omega - \mathrm{E})$ broadens the absorption and recombination spectra. This linewidth broadening can be classified as inhomogeneous broadening, typically caused by statistical fluctuations in chemical composition, alloy stoichiometry or thickness variations in quantum well/quantum wire/quantum dot systems, and as homogeneous broadening (or collision broadening), which is mainly related to carrier-carrier scattering and carrier-phonon scattering. In the case of inhomogeneous broadening, the lineshape function is typically a Gaussian function[16,17], while for homogeneous broadening, the lineshape function is a Lorentzian function[17–19]. When the two mechanisms contribute to linewidth broadening, the overall line shape is the convolution of the individual functions and is represented by Voigt integral. Since we are only interested in the overall broadening effect, we fit the measured PL spectra using Eq. 5 and Eq. 6 independently. Moreover, estimating the contribution of each mechanism to the final broadening width is beyond the scope of this work. As a result, we attribute the broadening width by Γ_{opt} to be either Γ_{Lorr} or Γ_{Gauss}, depending on the linewidth function used. The coefficients used in Eq. 1 - 3, such as the momentum matrix element and the reduced effective masses in Ge, are taken from the literature[15]. The Fermi-Dirac functions $\mathrm{f_c}$ and $\mathrm{f_v}$ in Eq. 1 and Eq. 2 are dependent on the carrier concentration, which is dependent on the dopant concentration shown in Table I and on the photo-excited carrier concentration. The photo-excited carrier concentrations are estimated by solving a steady state solution of the carrier transport continuity equation[21], where a radiative recombination coefficient ($\mathrm{R}^{\Gamma_c\Gamma_v} = 10^{-10}$ $\mathrm{cm^3s^{-1}}$) and Auger recombination coefficient ($\mathrm{C} = 5\times10^{-31}$ $\mathrm{cm^6s^{-1}}$)) were considered[15,22,23]. Moreover, Shockley-Read-Hall carrier lifetimes (τ_c) of 3 ns and 0.3 ns were used for undoped and doped Ge respectively. These carrier lifetime values are supported by the pump-probe spectroscopy measurements presented later in this paper. The result from fitting the $\Gamma_c - \Gamma_v$ emission is shown in Fig. 1 with the extracted broadening width listed in Table I. Since the extracted Γ_{Lorr} and Γ_{Gauss} are close to each other, we conclude that $\Gamma_{\mathrm{opt}} = 10$ meV for undoped Ge and $\Gamma_{\mathrm{opt}} \geq 45$ meV for doped Ge. The extracted broadening width from undoped Ge is consistent with prior experiments on bulk Ge[16,24]. On the other hand, $\Gamma_{\mathrm{opt}} \geq 45$ meV is needed to match the spectral shape of PL emission from all doped Ge. This increased broadening is believed to be related to the presence of scattering channels associated to dopants, evidenced also by the presence of a $\mathrm{L_c} - \Gamma_v$ recombination peak in the PL spectra.

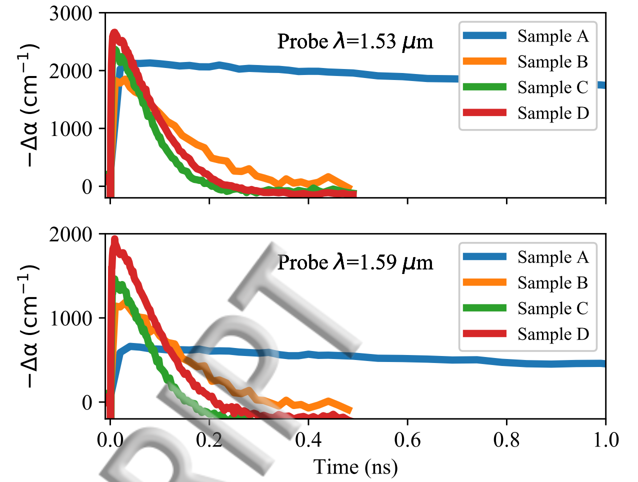

FIG. 2. Time resolved change in absorption coefficient of undoped and doped Ge measured at two different probe wavelengths for a pump intensity of 112 $\mathrm{mW/cm^2}$, which results in a photo-excited carrier concentration of $\sim 1.0\times10^{19}$ $\mathrm{cm^{-3}}$.

In addition to PL spectroscopy, pump-probe measurements were performed on the four Ge samples. Fig. 2 shows the time dependent change in absorption of the Ge films due to photo-excited carriers induced OBE and FCA, when Ge was pumped with a pumping intensity of 112 $\mathrm{mW/cm^2}$. The result shows the data extracted at different probe wavelengths, for undoped and doped Ge layers. Once the carriers are excited, the time necessary for them to scatter from the Γ to L conduction valley is around 230 fs. Beyond this time all injected carriers are redistributed over the two valleys due to thermalization, similar to what would happen under normal device operation. Therefore, in this work, we focus on the transient absorption spectra extracted 1 ps after the incidence of the pump pulse. When comparing the temporal responses of the different samples, it is evident that the carrier lifetime (τ_c) is an order of magnitude higher in undoped Ge (3 ns) as compared to all doped Ge films (< 3 ns). This behaviour was observed across a wide range of pump intensities. In undoped Ge-films, the carrier lifetime is typically limited by the defective Ge/Si interface[25,26]. However, the drop in lifetime from undoped Ge to doped Ge is related to dopants[9,10]. From the measurement results of Fig. 2, we extract the peak change in absorption coefficient ($-\Delta\alpha$), which represents the OBE. The resulting spectra are shown in Fig. 3 for all samples. Similar to what we observed for the PL spectra (Fig. 1), the OBE spectra of the doped samples are shifted towards longer wavelength due to dopant dependent bandgap narrowing. In addition, for all doped Ge films the OBE is suppressed and broadened with respect to that of undoped Ge. The modeling results with Γ_{opt} listed in Table I represent this trend as can be seen in Fig 3 for a wide range of pump intensities. This

ACCEPTED MANUSCRIPT

This manuscript was accepted by Appl. Phys. Lett. Click here to see the version of record.
AIP Publishing
ACCEPTED MANUSCRIPT

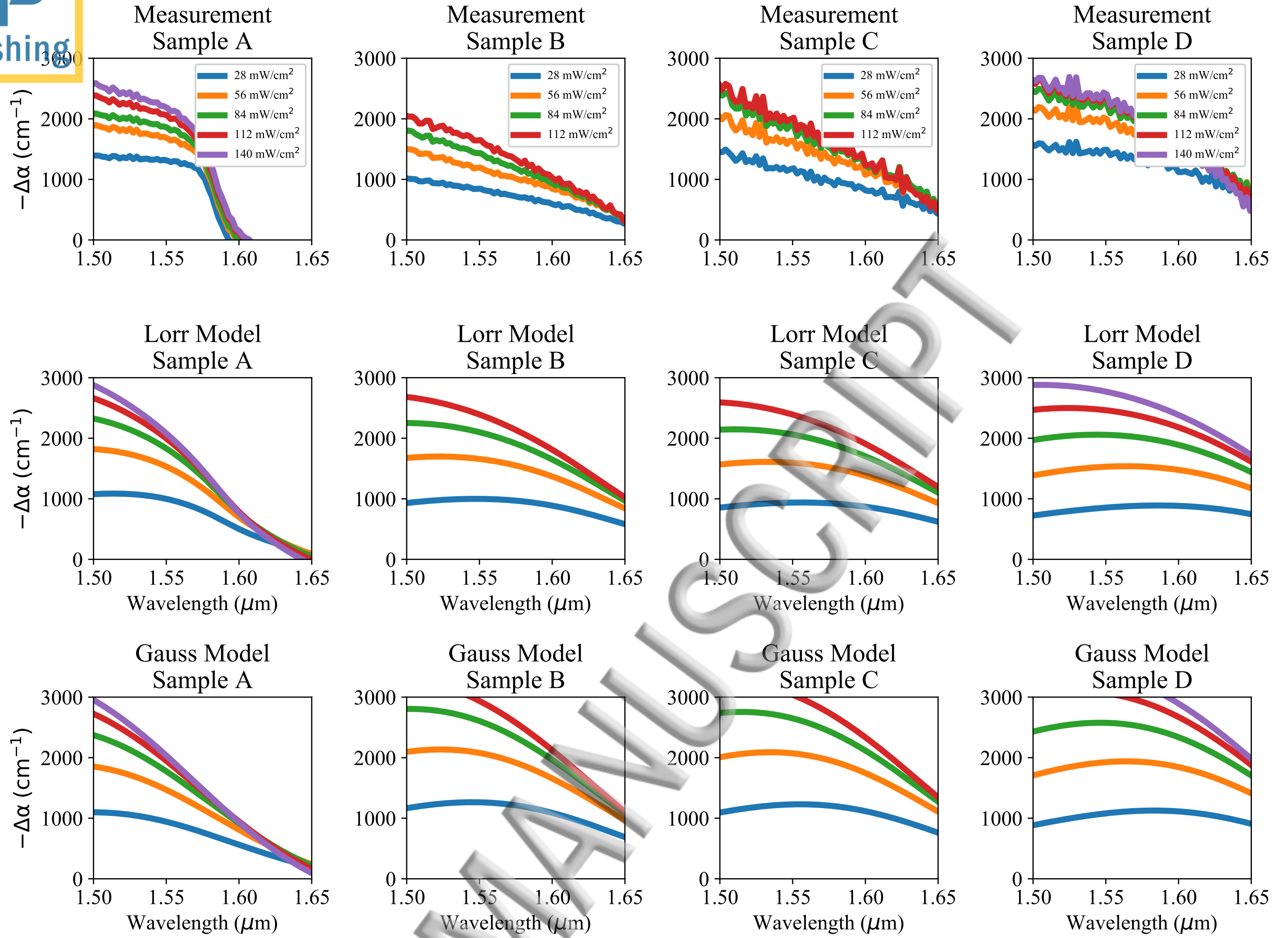

FIG. 3. The change in absorption coefficient ($-\Delta\alpha$) extracted from Fig. 2 for a wide range of pump intensity, which results in photo-excited carrier concentration of up to 1.0×10^{19} cm^{-3}. Modeling results of the change in absorption coefficient with the inclusion of linewidth broadening using Eq. 4-6. Note that $-\Delta\alpha = \alpha(\text{Unpumped}) - \alpha(\text{Pumped})$ is the change in absorption coefficient (or optical bleaching effect). This change in absorption coefficient is lower than the intrinsic absorption coefficient of Ge and therefore does not represent gain.

match between our experimental results and modeling data confirms that the carrier scattering events present in these layers are consistently observed in both the PL and pump-probe based experiments. To evaluate the impact on the device performance, modeling results with $\Gamma_{opt} \geq 45$ meV and carrier lifetime (τ_c) of < 0.3 ns in doped Ge with a doping level of 5.4×10^{19} cm^{-3} have a threshold current $> 40\times$ than that of doped sample with the same doping level but a linewidth broadening of 10 meV and a carrier lifetime (τ_c) of 3 ns (as for undoped Ge)[27,28].

In summary, we have studied the carrier scattering induced linewidth broadening effects in P-doped Ge films, by performing PL spectroscopy and femtosecond pump-probe spectroscopy. Due to linewidth broadening effects, we observed a significant increase in the full width at half maximum of the PL spectra and suppressed optical bleaching spectra for doped Ge when compared to undoped Ge. We extracted linewidth broadening $\Gamma_{opt} \geq 45$ meV for doped Ge and $\Gamma_{opt} = 10$ meV for undoped Ge by fitting the measured spectra with a density of states model. In addition, the carrier lifetime (τ_c) is lowered by more than one order of magnitude, from 3 ns in undoped Ge to ≥ 0.3 ns in P-doped Ge due to dopants. These results show that, despite these dopants are necessary to make Ge an efficient light emitter, they introduce detrimental scattering effects that strongly reduce the potential of realizing an energy efficient on-chip laser using P-doped Ge as the gain medium.

Yosuke Shimura acknowledges the Research Foundation of Flanders (FWO) for granting him a fellowship within the Pegasus Marie Curie Program. Pieter Geiregat acknowledges the FWO Vlaanderen for a postdoctoral fellowship. This work was supported by imec's

This manuscript was accepted by Appl. Phys. Lett. Click here to see the version of record.
AIP Publishing

industry-affiliation program on Optical I/O. Air Liquide Advanced Materials is acknowledged for providing Ge_2H_6.

[1] H. Chen, P. Verheyen, P. De Heyn, G. Lepage, J. De Coster, S. Balakrishnan, P. Absil, W. Yao, L. Shen, G. Roelkens, *et al.*, "-1 v bias 67 ghz bandwidth si-contacted germanium waveguide pin photodetector for optical links at 56 gbps and beyond," Optics Express **24**, 4622–4631 (2016).

[2] S. A. Srinivasan, M. Pantouvaki, S. Gupta, H. T. Chen, P. Verheyen, G. Lepage, G. Roelkens, K. Saraswat, D. Van Thourhout, P. Absil, *et al.*, "56 gb/s germanium waveguide electro-absorption modulator," Journal of Lightwave Technology **34**, 419–424 (2016).

[3] P. De Heyn, J. De Coster, P. Verheyen, G. Lepage, M. Pantouvaki, P. Absil, W. Bogaerts, J. Van Campenhout, and D. Van Thourhout, "Fabrication-tolerant four-channel wavelength-division-multiplexing filter based on collectively tuned si microrings," Journal of Lightwave Technology **31**, 3085–3092 (2013).

[4] D. Taillaert, F. Van Laere, M. Ayre, W. Bogaerts, D. Van Thourhout, P. Bienstman, and R. Baets, "Grating couplers for coupling between optical fibers and nanophotonic waveguides," Japanese Journal of Applied Physics **45**, 6071 (2006).

[5] M. Pantouvaki, S. Srinivasan, Y. Ban, P. De Heyn, P. Verheyen, G. Lepage, H. Chen, J. De Coster, N. Golshani, S. Balakrishnan, *et al.*, "Active components for 50 gb/s nrz-ook optical interconnects in a silicon photonics platform," Journal of Lightwave Technology **35**, 631–638 (2017).

[6] Y. Shimura, S. A. Srinivasan, D. Van Thourhout, R. Van Deun, M. Pantouvaki, J. Van Campenhout, and R. Loo, "Enhanced active p doping by using high order ge precursors leading to intense photoluminescence," Thin Solid Films **602**, 56–59 (2016).

[7] R. E. Camacho-Aguilera, Y. Cai, N. Patel, J. T. Bessette, M. Romagnoli, L. C. Kimerling, and J. Michel, "An electrically pumped germanium laser," Optics express **20**, 11316–11320 (2012).

[8] R. Koerner, M. Oehme, M. Gollhofer, M. Schmid, K. Kostecki, S. Bechler, D. Widmann, E. Kasper, and J. Schulze, "Electrically pumped lasing from ge fabry-perot resonators on si," Optics express **23**, 14815–14822 (2015).

[9] M. R. Barget, M. Virgilio, G. Capellini, Y. Yamamoto, and T. Schroeder, "The impact of donors on recombination mechanisms in heavily doped ge/si layers," Journal of Applied Physics **121**, 245701 (2017).

[10] Y. Yamamoto, L.-W. Nien, G. Capellini, M. Virgilio, I. Costina, M. A. Schubert, W. Seifert, A. Srinivasan, R. Loo, G. Scappucci, *et al.*, "Photoluminescence of phosphorus atomic layer doped ge grown on si," Semiconductor Science and Technology **32**, 104005 (2017).

[11] L. Ding, A. E.-J. Lim, J. T.-Y. Liow, M. Yu, and G.-Q. Lo, "Dependences of photoluminescence from p-implanted epitaxial ge," Optics express **20**, 8228–8239 (2012).

[12] R. Camacho-Aguilera, Z. Han, Y. Cai, L. C. Kimerling, and J. Michel, "Direct band gap narrowing in highly doped ge," Applied Physics Letters **102**, 152106 (2013).

[13] M. Oehme, M. Gollhofer, D. Widmann, M. Schmid, M. Kaschel, E. Kasper, and J. Schulze, "Direct bandgap narrowing in ge leds on si substrates," Optics express **21**, 2206–2211 (2013).

[14] S. L. Chuang, *Physics of photonic devices*, Vol. 80 (John Wiley & Sons, 2012).

[15] J. Liu, X. Sun, D. Pan, X. Wang, L. C. Kimerling, T. L. Koch, and J. Michel, "Tensile-strained, n-type ge as a gain medium for monolithic laser integration on si," Optics express **15**, 11272–11277 (2007).

[16] V. R. D'Costa, Y. Fang, J. Mathews, R. Roucka, J. Tolle, J. Menéndez, and J. Kouvetakis, "Sn-alloying as a means of increasing the optical absorption of ge at the c-and l-telecommunication bands," Semiconductor Science and Technology **24**, 115006 (2009).

[17] L. Pavesi and M. Guzzi, "Photoluminescence of al x ga1- x as alloys," Journal of Applied Physics **75**, 4779–4842 (1994).

[18] S. M. Sze and K. K. Ng, *Physics of semiconductor devices* (John wiley & sons, 2006).

[19] M. Virgilio, D. Sabbagh, M. Ortolani, L. Di Gaspare, G. Capellini, and M. De Seta, "Physical mechanisms of intersubband-absorption linewidth broadening in s-ge/sige quantum wells," Physical Review B **90**, 155420 (2014).

[20] J. Singh, *Electronic and optoelectronic properties of semiconductor structures* (Cambridge University Press, 2007).

[21] M. Virgilio, C. Manganelli, G. Grosso, T. Schroeder, and G. Capellini, "Photoluminescence, recombination rate, and gain spectra in optically excited n-type and tensile strained germanium layers," Journal of Applied Physics **114**, 243102 (2013).

[22] L. Carroll, P. Friedli, S. Neuenschwander, H. Sigg, S. Cecchi, F. Isa, D. Chrastina, G. Isella, Y. Fedoryshyn, and J. Faist, "Direct-gap gain and optical absorption in germanium correlated to the density of photoexcited carriers, doping, and strain," Physical review letters **109**, 057402 (2012).

[23] R. Geiger, T. Zabel, E. Marin, A. Gassenq, J.-M. Hartmann, J. Widiez, J. Escalante, K. Guilloy, N. Pauc, D. Rouchon, *et al.*, "Uniaxially stressed germanium with fundamental direct band gap," arXiv preprint arXiv:1603.03454 (2015).

[24] R. Geiger, *Direct Band Gap Germanium for Si-compatible Lasing*, Ph.D. thesis (2016).

[25] R. Geiger, J. Frigerio, M. Süess, D. Chrastina, G. Isella, R. Spolenak, J. Faist, and H. Sigg, "Excess carrier lifetimes in ge layers on si," Applied Physics Letters **104**, 062106 (2014).

[26] S. A. Srinivasan, M. Pantouvaki, P. Verheyen, G. Lepage, P. Absil, J. Van Campenhout, and D. Van Thourhout, "Extraction of carrier lifetime in ge waveguides using pump probe spectroscopy," Applied Physics Letters **108**, 211101 (2016).

[27] A. Ghrib, M. El Kurdi, M. Prost, S. Sauvage, X. Checoury, G. Beaudoin, M. Chaigneau, R. Ossikovski, I. Sagnes, and P. Boucaud, "All-around sin stressor for high and homogeneous tensile strain in germanium microdisk cavities," Advanced Optical Materials **3**, 353–358 (2015).

[28] M. Prost, M. El Kurdi, F. Aniel, N. Zerounian, S. Sauvage, X. Checoury, F. Bœuf, and P. Boucaud, "Analysis of optical gain threshold in n-doped and tensile-strained germanium heterostructure diodes," Journal of Applied Physics **118**, 125704 (2015).

ACCEPTED MANUSCRIPT

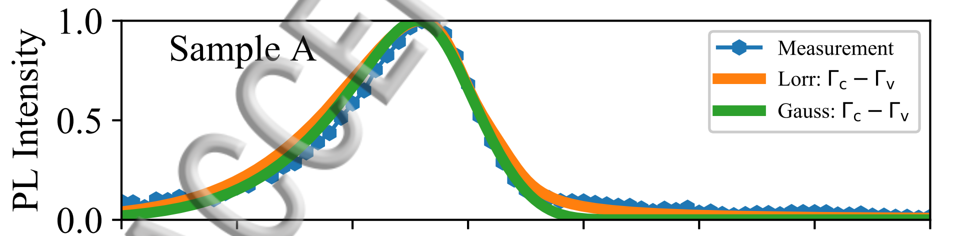
Sample A
Measurement
Lorr: $\Gamma_c - \Gamma_v$
Gauss: $\Gamma_c - \Gamma_v$
PL Intensity
1.0
0.5
0.0
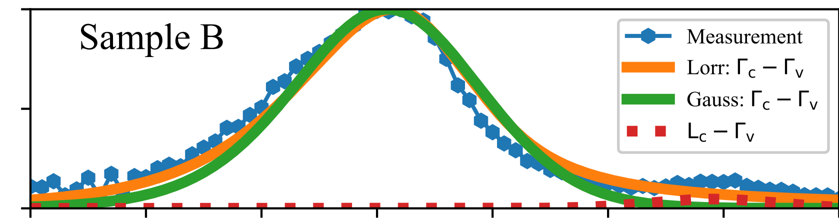
Sample B
Measurement
Lorr: $\Gamma_c - \Gamma_v$
Gauss: $\Gamma_c - \Gamma_v$
$L_c - \Gamma_v$
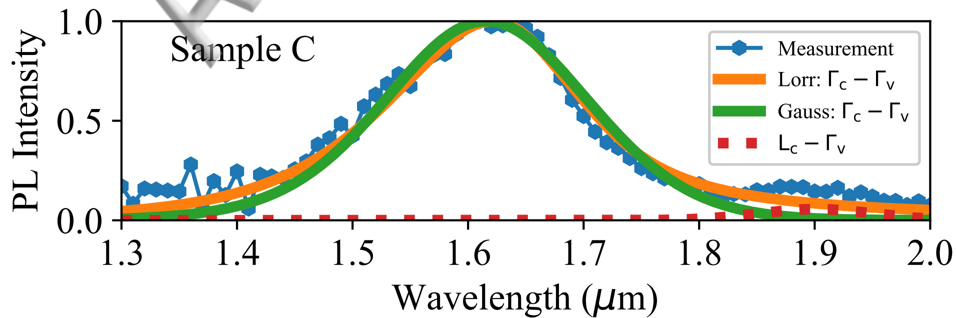
Sample C
Measurement
Lorr: $\Gamma_c - \Gamma_v$
Gauss: $\Gamma_c - \Gamma_v$
$L_c - \Gamma_v$
PL Intensity
1.0
0.5
0.0
1.3 1.4 1.5 1.6 1.7 1.8 1.9 2.0
Wavelength (μm)
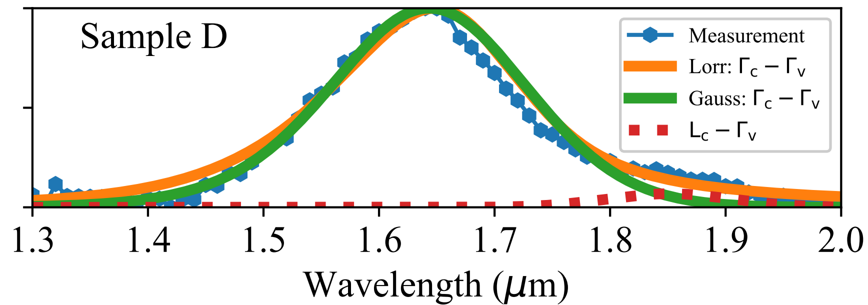
Sample D
Measurement
Lorr: $\Gamma_c - \Gamma_v$
Gauss: $\Gamma_c - \Gamma_v$
$L_c - \Gamma_v$
1.3 1.4 1.5 1.6 1.7 1.8 1.9 2.0
Wavelength (μm)

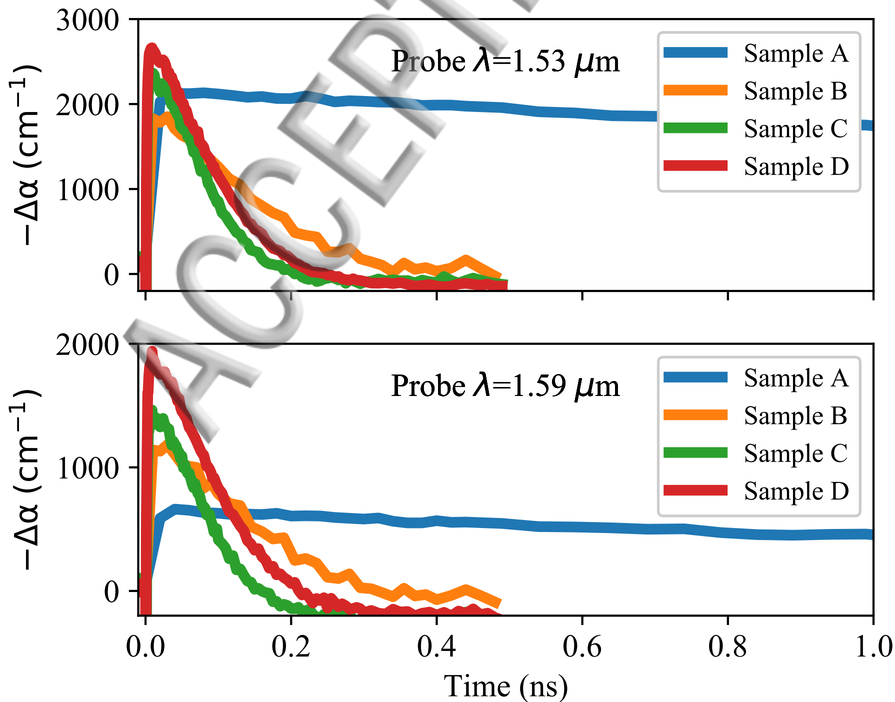
Probe λ=1.53 μm
Sample A
Sample B
Sample C
Sample D
3000
2000
1000
0
−Δα (cm⁻¹)
Probe λ=1.59 μm
Sample A
Sample B
Sample C
Sample D
2000
1000
0
−Δα (cm⁻¹)
0.0
0.2
0.4
0.6
0.8
1.0
Time (ns)
ACCEPTED

Measurement
Sample A

$-\Delta\alpha\ (\mathrm{cm}^{-1})$

0, 1000, 2000, 3000

1.50, 1.55, 1.60, 1.65

28 mW/cm^2
56 mW/cm^2
84 mW/cm^2
112 mW/cm^2
140 mW/cm^2

Measurement
Sample B

28 mW/cm^2
56 mW/cm^2
84 mW/cm^2
112 mW/cm^2

Measurement
Sample C

28 mW/cm^2
56 mW/cm^2
84 mW/cm^2
112 mW/cm^2

Measurement
Sample D

28 mW/cm^2
56 mW/cm^2
84 mW/cm^2
112 mW/cm^2
140 mW/cm^2

Lorr Model
Sample A

Lorr Model
Sample B

Lorr Model
Sample C

Lorr Model
Sample D

Wavelength (μm)

Gauss Model
Sample A

Gauss Model
Sample B

Gauss Model
Sample C

Gauss Model
Sample D

Wavelength (μm)

ACCEPTED MANUSCRIPT